Production of fiberboards from shives collected after continuous fiber mechanical extraction from oleaginous flax

Philippe Evon, Benjamin Barthod-Malat, Marie Grégoire, Guadalupe Vaca Medina, Laurent Labonne, Stéphane Ballas, Thierry Véronèse, Pierre Ouagne

Production of fiberboards from shives collected after continuous fiber mechanical extraction from oleaginous flax

Philippe Evon[a], Benjamin Barthod-Malat[a,b], Marie Grégoire[b], Guadalupe Vaca-Medina[a,d], Laurent Labonne[a], Stéphane Ballas[c], Thierry Véronèse[c], and Pierre Ouagne[b]

[a]Laboratoire de Chimie Agro-industrielle (LCA), Université de Toulouse, ENSIACET, INRA, INPT, Toulouse Cedex 4, France; [b]Laboratoire Génie de Production (LGP), Université de Toulouse, ENIT, INPT, Tarbes Cedex, France; [c]Ovalie Innovation, Auch, France; [d]Centre d'Application et de Traitement des Agroressources (CATAR), Université de Toulouse, INPT, Toulouse, France

ABSTRACT

In this study, fiberboards were produced from shives collected after continuous fiber mechanical extraction from oleaginous flax straw. Fiberboards were produced through thermo-pressing, and their mechanical and thermomechanical properties were studied, as well as their water resistance. The influence of two pretreatments for shives and lignin addition was investigated on the different properties. Boards obtained were all cohesive hardboards. The optimal board was obtained from fibers extruded from the shives and without addition of any supplementary lignin amount. Looking at its characteristics and standard NF EN 312, the latter perfectly complied with the requirements for type P1 boards, i.e., boards for general uses in dry conditions.

KEYWORDS

Oleaginous flax shives; thermomechanical fiber extraction; twin-screw extruder; lignocellulosic fibers; thermo-pressing; fiberboards

摘要

在这项研究中，纤维板从连续纤维机械提取油脂亚麻秸秆收集后产生的碎片。通过热压制备了纤维板，研究了它们的力学性能和热机械性能以及耐水性。对粗纤维、木质素添加量对不同性质的两种预处理的影响研究。板均粘结硬质纤维板。最佳板获得纤维挤压从和没有任何补充木质素添加量。鉴于其特点和标准NF EN 312，后者完全符合P1型板的要求，即在干燥条件下一般用途板。

关键词

油脂亚麻屑; 热机械纤维萃取; 双螺杆挤出机; 木质纤维素纤维; 热压; 纤维板

Introduction

Oleaginous flax is cultivated primarily for its seeds. Seeds can contain up to 45% of vegetal oil with α-linolenic acid (C18:3 ω-3) (56%), linoleic acid (C18:2 n-6) (16%), and oleic acid (C18: 1 n-9) (18%). Thus, linseed oil is an important vegetal source of omega-3 and omega-6 fatty acids. Therefore, it is widely recommended for human consumption. It can be also used for the formulation of many cosmetic products because of its nourishing properties. Lastly, because linseed oil cures spontaneously in air, it is also used frequently as a siccative in several industrial sectors, e.g., vegetable inks, oil paints, floor cleaners, and wood preservatives.

Around 11,000 ha/year of oleaginous flax are cultivated in France (ADEME 2011). In parallel, the worldwide production was about 1.7 Mha in 2009, Canada being the main producer (650,000 ha). The amount of straw is about 2 t/ha. Some specific varieties can even generate up to 5.5 t/ha straw without any negative effect in their seed yield (Rennebaum et al. 2002). The straw of oleaginous flax

CONTACT Philippe Evon Philippe.Evon@ensiacet.fr Laboratoire de Chimie Agro-industrielle (LCA), Université de Toulouse, ENSIACET, INRA, INPT, 4 allée Émile Monso, 31030 Toulouse Cedex 4, France.

is poorly valued, and this is the reason why it is considered as a by-product for the oleaginous flax cultivation. However, a few studies revealed quite promising mechanical properties for the linseed individual fibers (Pillin et al. 2011; Rennebaum et al. 2002; Tomljenovic and Erceg 2016), which in turn would make possible to envisage their use for the production of reinforcement textiles for structural or semi-structural composite applications. Developing a continuous mechanical process for the extraction of fibers from oleaginous flax stems thus appears as an interesting challenge for the years to come.

A recent study suggested the use of an "all fiber" extraction equipment to conduct continuously and at a semi-industrial scale (a raw material inlet flow rate of approximately 175 kg/h) the extraction of fibers from oleaginous flax straw (Ouagne et al. 2017). In this study, two different dew-retting levels and two degrees of stem rewetting before fiber extraction were tested. In all cases, the amount of extracted fibers (i.e., 38–40% of the stem dry mass) was much higher than what was found in previous studies using also oleaginous flaw straw (Pillin et al. 2011; Rennebaum et al. 2002; Tomljenovic and Erceg 2016), and it was perfectly comparable to that of textile flax. In addition, depending on the operation conditions used, diameter of extracted fibers was ranging from about 20 to 24 μm and their tensile strength average value varied from 324 to 377 MPa. Such properties were reduced by about 50% compared with values measured from fibers manually extracted (Pillin et al. 2011). However, they were situated in the lower part of the textile flax range. Lastly, the mean length of individual fibers was 5.1–5.3 cm when liquid water was added to the stem immediately before fiber extraction. In conclusion, looking at those mechanical and dimensional characteristics, fibers extracted mechanically from oleaginous flax straw would be suitable for the production of carded aligned fiber yarns for technical reinforcing textiles (e.g., semi-structural composite parts or geotextiles).

Results from Ouagne and coworkers demonstrated the economic interest and the potential added value of harvesting the oleaginous flax stems for technical fiber applications (Ouagne et al. 2017). Such extraction process generated at the same time two other vegetal fractions of interest: a vegetal dust and shives. On the one hand, vegetal dust consisted in small particles (i.e., fines) which could potentially be used for the mechanical reinforcement of thermoplastic polymers (Gamon, Evon, and Rigal 2013). On the other hand, oleaginous flax shives were evacuated by gravity. Shives are the ligneous part of flax stems. As for shives from textile flax, they could be used as animal litters because of their high water absorbency. However, looking at their high lignocellulose content and at their resulting promising thermal insulation properties, they would be also usable (1) as reinforcing fillers inside wood-polymer composites (Gamon, Evon, and Rigal 2013), (2) for the manufacture of insulation materials using hot pressing (Evon et al. 2014a) or compression molding (Evon et al. 2015a), or (3) as bio-aggregates for the design of bio-based insulating concretes (Gazagnes, Magniont, and Escadeillas 2009).

Another possible use of oleaginous flax shives could be the production of high-density self-bonded fiberboards using hot pressing, with cellulosic fibers and lignins potentially acting as mechanical reinforcement and natural binder, respectively. By-products originating from sunflower and coriander cultivations (i.e., stalk and straw, respectively) were already used for the manufacture of hardboards using thermo-pressing (Evon et al. 2015b; Uitterhaegen et al. 2017). In addition, because shives reveal naturally high lignin content, this ligneous part could contribute to self-bonding, giving the opportunity to obtain cohesive materials without any (synthetic) resin addition. Self-bonded hardboards from sunflower cakes (Evon et al. 2015b), coriander fruits (Uitterhaegen et al. 2016a, 2017), or jatropha seeds (Evon, Amalia Kartika, and Rigal 2014b) were already produced with success thanks to the protein-based fraction inside the starting materials acting as natural binder. For oleaginous flax shives, it is reasonable to assume that lignins inside shives could act in that case as the natural binder. Indeed, lignins can be used as a natural binder through thermo-pressing, the mobilization of this lignin-based binder needing high temperature and pressure during hot pressing (Tajuddin, Ahmad, and Ismail 2016). This results in the production of binderless boards, thus avoiding the use of any chemical additives. Moreover, more lignins can be added to the

starting material before molding when necessary, i.e., when its lignin content is insufficient (Theng et al. 2018).

Among the first commercially available lignin-bonded fiberboards, it is possible to cite Masonite (USA) and Isorel (France) boards. Available since the beginning of the twentieth century, these products are in the form of hardboards made from wood fibers. Their production is conducted thanks to a wet method and under high pressure, not requiring the addition of any synthetic binder containing formaldehyde. Lignin and hemicelluloses from fibers are first deactivated during the mechanical defibration of wood in the presence of water vapor. Then, they polymerize under the effect of temperature and pressure, esterification reactions allowing junctions with the cellulosic fibers and thus ensuring the board cohesion.

When producing binderless boards, different pretreatments are frequently proposed for increasing the auto-adhesion of natural fibers. One possible enhancement is the pretreatment of fibers using a phenol oxidase enzyme, e.g., laccase (Felby, Hassingboe, and Lund 2002; Felby, Pedersen, and Nielsen 1997; Felby et al. 2004). This was demonstrated with success by Felby and coworkers from beech wood (*Fagus sylvatica*) fibers. When boards are manufactured from laccase-treated fibers using hot pressing, this increases the inter-facial compatibility, thus enhancing the internal bonding in dry process boards (Felby et al. 2004). Felby and coworkers claimed that the use of lignin-oxidizing enzymes contributed to the generation of phenoxy radicals in lignin from the plant cell wall by oxidation, these stable radicals causing cross-linking or loosening of the lignin structure. However, it could not be concluded if this lignin cross-linking is forming covalent bonds between fibers or if the polymerized loosely associated lignin works as an adhesive. As a result, fiberboards bonded by laccase catalyzed oxidation revealed comparable strength properties to those of boards bonded by a conventional UF resin, offering at the same time a process more respectful of the environment and with reduced health hazards (Felby, Hassingboe, and Lund 2002; Felby et al. 2004). In addition, such laccase treated boards were made successfully in a pilot-scale process simulating continuous full-scale industrial production (Felby, Hassingboe, and Lund 2002). Nonetheless, this required higher pressing temperatures and longer pressing times, which in turn could be a disadvantage from an economic point of view.

Steam explosion (Anglès et al. 2001; Anglès et al. 1999; Quintana et al. 2009; Velásquez et al. 2003; Xu et al. 2006) and thermomechanical defibration in the presence of water using twin-screw extrusion (Theng et al. 2017, 2018; Uitterhaegen et al. 2017) are two other promising pretreatments for increasing the performances of binderless boards, in particular their mechanical resistance and dimensional stability. In both processes, the fiber structure disrupts, liberating lignins from the inner cell wall to the fiber surface (Pintiaux et al. 2015; Tajuddin, Ahmad, and Ismail 2016). Hemicelluloses can hydrolysate simultaneously, as well as lignins in a smaller proportion. The resulting increased lignin accessibility contributes to better self-bonding during thermo-pressing. In addition, an improvement in the board water resistance can be also observed from such pretreatments (Anglès et al. 2001; Uitterhaegen et al. 2017; Velásquez et al. 2003). Lastly, defibration separates fibers from their neighbors. This results in an increase in their surface area. And, from a morphological point of view, their aspect ratio, defined as the ratio of fiber length to width, also increases, contributing to an improvement of their mechanical reinforcement ability (Anglès et al. 1999; Uitterhaegen et al. 2017; Xu et al. 2006).

In addition to extrusion refining, having fibers resulting from this pretreatment and also oriented before thermo-pressing could also have a positive effect on the reinforcing properties of the obtained fiberboard. The use of a sheet-forming apparatus from the paper-making techniques should allow such an orientation before hot pressing.

The aim of this study was to investigate the opportunity to produce cohesive fiberboards from oleaginous flax shives using hot pressing, and to study the influence of (1) two different pretreatments for shives (thermomechanical defibration through twin-screw extrusion and handsheet formation from extruded shives) and (2) lignin addition on the characteristics of fiberboards.

Materials and methods

Materials

Shives used in this study (Figure 1(a)) originated from a single batch of oleaginous flax (*Linum usitatissimum* L.) straw of Everest variety. Oleaginous flax was cultivated in the South West part of France. Straw was non-retted, i.e., packed into 200 kg balls immediately after the seed harvesting (beginning of July).

Biolignin™ was supplied by CIMV (France). It was in the form of a brown color powder. It was extracted from wheat straw thanks to an organosolv process that used a mixture of acetic acid and formic acid as extracting solvent. Lignin purity in the final product (Biolignin™) was 89% of the dry matter.

Analytical methods

Moisture contents were determined according to French standard NF V 03-903. Mineral contents were determined according to French standard NF V 03-322. The three parietal constituents inside shives, i.e., cellulose, hemicelluloses, and lignins, were estimated thanks to the ADF-NDF method of Van Soest and Wine (1967, 1968). Lastly, water-soluble compounds were determined by measuring the mass loss of the test sample after 1 h in boiling water. All determinations were carried out in duplicate.

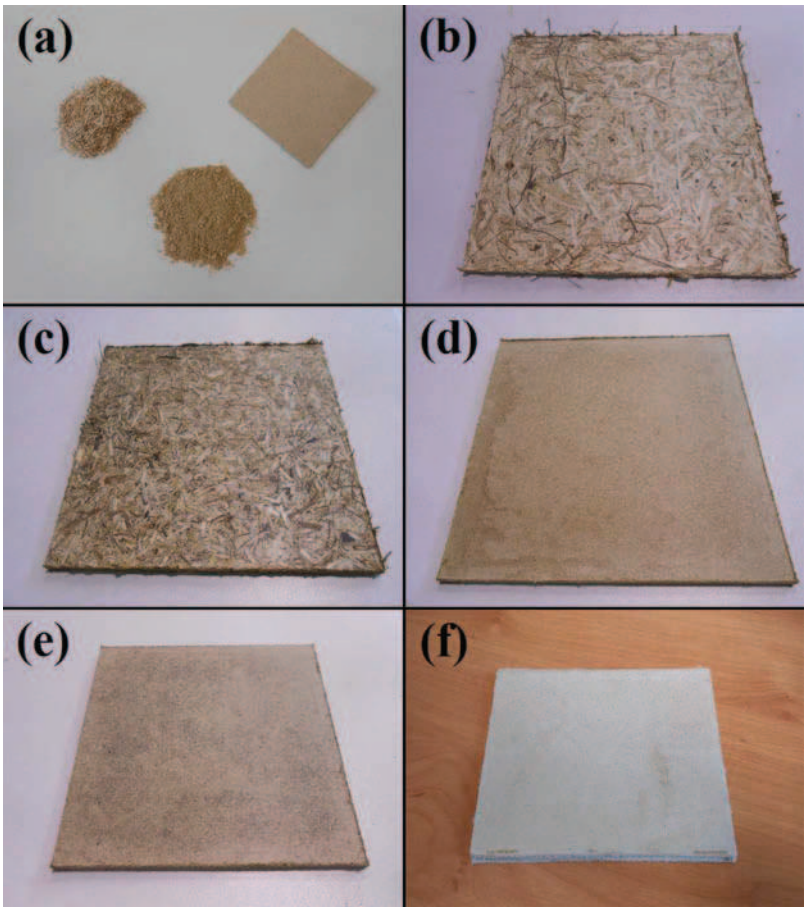

Figure 1. Photographs of (a) starting materials used for thermo-pressing (i.e., raw shives, extruded shives and handsheet obtained from extruded shives, from left to right), (b) RS board, (c) RSL board, (d) ES board, (e) ESL board, and (f) HS board.

Dynamic vapor sorption analysis

Oleaginous flax straw shives and technical fibers were analyzed through dynamic vapor sorption (DVS) analysis. The latter was performed using a DVS Advantage (Surface Measurement Systems Ltd., UK) automated gravimetric vapor sorption analyzer. The uptake of vapor was measured gravimetrically thanks to a Cahn D200 recording ultramicrobalance having a mass resolution of ±0.1 μg. A mixing of saturated and dry carrier gas streams using mass flow controllers allowed an effective control of relative humidity around the sample. Experiments were performed at 25°C and a temperature-controlled incubator enclosing the entire system maintained this temperature constant (±0.1°C). For each experiment, the sample was placed into the DVS analyzer under a continuous stream of dry air (<0.1% RH). Test sample mass was around 10 mg. Prior to exposure to any water vapor, samples were dried at 103°C and 0% RH to remove adsorbed water. A dry baseline mass could thus be established. Samples were subjected to a water adsorption procedure following the next relative humidity profile: 0%, 15%, 30%, 45%, 60%, 75%, and 90% RH. For each relative humidity value, an equilibrium of the sample mass was reached before any increase of the relative humidity. After reaching the equilibrium at 90% RH, samples were also subjected to a water desorption procedure, using a decreasing relative humidity profile: 90%, 75%, 60%, 45%, 30%, 15%, and 0% RH. From the complete moisture sorption profile, an isotherm was then plotted using the DVS Advanced Analysis Suite v3.6 software.

Thermomechanical pretreatment of shives through twin-screw extrusion

Shives were subjected to a thermomechanical defibration pretreatment through twin-screw extrusion using a Clextral (France) Evolum HT 53 machine with eight modules. Before extrusion, their moisture content was 10.4%. The screw profile used was the same as the one previously optimized for defibration of rice straw (Theng et al. 2017) and coriander straw (Uitterhaegen et al. 2017). The inlet flow rate of shives was 15.0 kg/h. In parallel, water was injected at the end of module 3 using a piston pump at a 15.0-kg/h inlet flow rate, corresponding to a 1.0 liquid/solid (L/S) ratio during refining. Screw rotation speed was 150 rpm, and temperature along the barrel varied from 110°C at the level of water injection to 100°C at the outlet. To avoid any proliferation of fungi and molds at storage, extruded shives (Figure 1(a)) were dried at 60°C in a ventilated oven until reaching approximately 10% moisture content.

Handsheet formation from extruded shives

Handsheets were obtained from extruded shives using a TechPap (France) ADF Automated Dynamic handsheet Former. Extruded shives were diluted inside water using a 15-g/L concentration. A commercial cellulose pulp from wood was also added at a 2.5-g/L concentration to generate a sheet with better cohesion. The obtained suspension was then projected at the inner periphery of a rotating cylindrical jar covered with a bronze wire. Projection was accomplished using a 25–20 injector nozzle fixed at the end of a delivery metal tube moving vertically up and down. The wire speed was voluntarily chosen to be much greater than the jet one so as to parallelize the fibers. Rectangular handsheets produced (Figure 1(a)) were thus orientated. After forming, they were removed from the cylindrical jar and then dried in a ventilated oven at 60°C.

Morphological analyzes

The morphological analysis of raw shives was performed by image analysis using the ImageJ (USA) software. It was performed from a sample containing about 3000 particles. These were first deposited on a plastic film and the latter was placed on a Toshiba (Japan) e-Studio 257 scanner. Then, a scan was realized in gray level using a 600 dots per inch (dpi) resolution. ImageJ software was used with a

threshold of between 60 and 85 so as to get an image with all particles visible and clean-cut in the photograph. Their length, width, and aspect ratio (defined as the ratio of length to width) were then measured automatically. Results were expressed as mean value ± standard deviation.

The morphological analysis of extruded shives was conducted using a TechPap (France) MorFi Compact analyzer. For each experiment, about 15,000 particles were analyzed, and this allowed the determination of the average length, the average diameter, and the average aspect ratio of fibers, as well as the fines percentage. Determinations were carried out in triplicates.

Apparent and tapped densities

Apparent and tapped densities of shives were determined before and after extrusion refining. Tapped density was measured using a Granuloshop (France) Densitap ETD-20 volumenometer. Apparent density was obtained before compaction. Determinations were carried out in triplicates.

Thermogravimetric analysis measurements

Shives before and after twin-screw extrusion refining were analyzed through thermogravimetric analysis (TGA). Measurements were conducted using a Shimadzu TGA-50 (Japan) analyzer. Dynamic analysis was conducted under air at a heating rate of 5°C/min, from 20 to 750°C. Before analyzing them, samples were placed in a climatic chamber (60% RH, 25°C) for 3 weeks to reach an equilibrium state. Test sample mass was about 5 mg. Sample weight was measured as a function of the increasing temperature. Subsequently, data were used to plot the percentage of undegraded sample as a function of the temperature. Determinations were carried out in duplicates.

Thermo-pressing

Raw shives, extruded shives, handsheets, and Biolignin™ were all dried in a ventilated oven (60°C, 12 h) to minimize vapor generation during thermo-pressing. Such drying thus reduced the risk of defects like blisters inside fiberboards (Evon, Amalia Kartika, and Rigal 2014b; Evon et al. 2015b; Uitterhaegen et al. 2016a, 2017). Their moisture contents at molding were 3.7%, 3.5%, 4.1%, and 3.2%, respectively. A 400-t capacity Pinette Emidecau Industries (France) heated hydraulic press was then used for thermo-pressing. Molding was conducted inside an aluminum mold, thus leading to the production of 150 mm × 150 mm fiberboards. For all experiments, the used thermo-pressing process parameters were always the same, i.e., 150 s time, 200°C temperature, and 19.7 MPa pressure. In addition, the quantity of shives was always 100 g (i.e., 444.4 mg/cm^2). Lastly, when lignin was added, a 25-g mass was used, corresponding to a 25% mass content in proportion to shives. Fiberboards were obtained from raw shives with and without Biolignin™ added, from extruded shives with and without Biolignin™ added, and from handsheets without Biolignin™ added. This contributed to the production of five different board types named RS, RSL, ES, ESL, and HS, respectively. In the case of HS board, 18 handsheets were superimposed on each other before molding so as to respect the 100-g initial mass.

For each board type, three fiberboards were produced. First, they were equilibrated in a climatic chamber (60% RH, 25°C) for 3 weeks. For each characteristic measured, test specimens were cut from the same fiberboard, meaning that the obtained data (including mean value and standard deviation) illustrated a variation in one board. After equilibration, a first fiberboard was used to determine thickness, mean apparent density, and bending properties. Four 30 mm wide and 130 mm long-test specimens were cut. Their thickness was then measured at three points and their length at two points. Thickness (t) and length (l) mean values were recorded to calculate the specimen volume, and test specimens were all weighed to calculate their density (d). Thickness and mean apparent density of fiberboard were the mean values of measurements made on the four test specimens. A second fiberboard was used for measuring: impact strength, surface hardness, and

finally thermomechanical properties. The third fiberboard was used for measuring internal bond strength, thickness swelling (TS), and finally water absorption (WA).

Bending properties

Bending properties of fiberboards were measured using French standard NF EN 310. Measurements were conducted according to the three points bending technique using an Instron 33R4204 (USA) universal testing machine. During flexural test, a 500-N load cell, a 2-mm/min test speed, and an 80-mm grip separation were used. The measured properties were the load (F) at failure, the flexural strength (σ_f), and the elastic modulus (E_f). All determinations were carried out four times.

Charpy impact strength

Impact strength of fiberboards was determined according to French standard NF EN ISO 179 from eight unnotched test specimens, using the three points bending technique and a 25-mm grip separation. Tests were conducted at 23°C using a Testwell Wolpert 0–40 da N cm (France) Charpy machine. This resulted in the determination of absorbed energy (W) and resilience (K). After fiberboard equilibration, the test specimens used for analysis were cut. They were 15 mm wide and 60 mm long. Their section was calculated after measuring thickness at three points, resulting in a mean value (t). All determinations were carried out eight times.

Internal bond strength

Internal bond strength (IB) of optimal fiberboard was determined according to standard ISO 16984:2003 from four test specimens. Test samples were 50 mm × 50 mm squares. Tests were made using an Instron 33R4204 (USA) universal testing machine fitted with a 5000-N load cell. A 5-mm/min test speed was applied. Determinations were carried out in quadruplicates.

Shore D surface hardness

Shore D surface hardness of fiberboards was measured according to French standard NF EN ISO 868 using a Bareiss (Germany) durometer. All determinations were carried out 48 times for each fiberboard (24 times for each side).

TS and WA

Four 50 mm × 50 mm samples were used to measure the TS and the WA of fiberboards. Samples were submerged in water at 25°C for 24 h. TS was determined according to French Standard NF EN 317. For this, thickness of each sample was measured at four points before and after soaking in water. Each sample was also weighed before and after soaking to determine WA. Determinations were carried out in quadruplicates.

Dynamic mechanical thermal analysis

The thermomechanical behavior of fiberboards was evaluated from dynamic mechanical thermal analysis (DMTA) analysis. DMTA experiments were conducted using a Triton Technology Tritec 2000 (UK) machine. For each tested fiberboard, the two different specimens used for analysis were 10 mm wide and 30 mm long. Measurements were made using the single cantilever mode and next operating conditions: 1 Hz frequency, 50 µm displacement, and a 3-C/min heating rate from −50 to 165°C. Distance between the two points was 10 mm. Curves for storage modulus (E') and loss factor (tan δ) were plotted. Two samples were tested for each fiberboard.

Statistical analyses

Mechanical properties, TS and WA of the five fiberboards manufactured by thermo-pressing are expressed as the mean ± the standard deviation. For each board property, means were compared by the use of a one-way analysis of variance (ANOVA). Individual means were compared using the Duncan's multiple range test at a 5% probability level.

Results and discussion

Physicochemical characteristics of non pretreated and pretreated shives

A recent study consisted in extracting mechanically fibers from oleaginous flax straw using an "all fiber" equipment (Ouagne et al. 2017). It resulted in the production of three fractions: (1) a fiber lap (i.e., technical fibers), (2) shives (Figure 1(a)), and (3) fines (i.e., vegetal dust). When conducted from non-retted straw, the latter being rewetted by sprinkling liquid water before the extraction of fibers, dry weights of these three fractions were 56.0, 38.3, and 5.7 kg, respectively, for 100 kg dry matter straw at the inlet. In addition, the lap purity in technical fibers was 72.1% in mass. Chemical compositions of the two main fractions, i.e., shives and technical fibers, are presented in Table 1. Cellulose content was much more important inside technical fibers than inside shives (78.7% of the dry matter instead of 45.6%). On the contrary, contents for hemicelluloses and especially lignins were higher inside shives, the ligneous part of oleaginous flax straw: 22.4% instead of 7.0%, and 25.1% instead of 2.5%, respectively.

Moisture content of equilibrated shives, i.e., after conditioning in a climatic chamber (60% RH, 25°C) for 3 weeks, appeared also a little higher than that of technical fibers: 8.4% instead of 7.8% (Table 1). This was confirmed from water sorption isotherm obtained by DVS measurements, where water vapor uptake at 25°C was higher for shives in the 30–90% relative humidity range (Figure 2). For the highest relative humidity value tested (i.e., 90% RH), the difference of water vapor uptakes was important: 18.3% for shives instead of only 16.4% for technical fibers. Even if shives contain more lignins which hydrophobic character is known as significant because of their structure made of phenolic compounds, they were therefore more sensitive to water vapor uptake than technical fibers. This could be a disadvantage for subsequent resistance to water of fiberboards from shives. The most likely reason for that could be the higher content of hemicelluloses inside shives, which are known to be amorphous polysaccharides with a quite high hygroscopic behavior. Conversely, even if cellulose is a biopolymer which contains many hydroxyl groups, its natural semi-crystallinity does not favor the adsorption of water molecules, thus contributing to a lower water vapor uptake of technical fibers. A higher sensitivity of shives to water was also evidenced during the DVS desorption cycle (i.e., from 90% to 0% RH), the latter being still performed at 25°C. Indeed, water vapor uptake remained systematically higher for shives compared with values observed for technical fibers (Figure 2). In particular, from values obtained for 0% RH, water desorption from technical fibers was complete at 25°C. Meanwhile, water vapor uptake was still 0.3% for shives, meaning that water desorption was incomplete in that case. Some water molecules were thus still adsorbed at the

Table 1. Chemical composition of shives and technical fibers generated after continuous fiber mechanical extraction from oleaginous flax straw.

Material	Shives	Technical fibers
Moisture (%)	8.4 ± 0.2	7.8 ± 0.0
Minerals (% of the dry matter)	2.0 ± 0.1	2.0 ± 0.1
Cellulose (% of the dry matter)	45.6 ± 0.4	79 ± 2
Hemicelluloses (% of the dry matter)	22.4 ± 0.1	7.0 ± 0.1
Lignins (% of the dry matter)	25.1 ± 0.6	2.5 ± 0.1
Water-soluble components (% of the dry matter)	4.1 ± 0.1	6.5 ± 0.5

Moisture contents were determined from equilibrated materials, i.e., after conditioning in a climatic chamber (60% RH, 25°C) for 3 weeks.

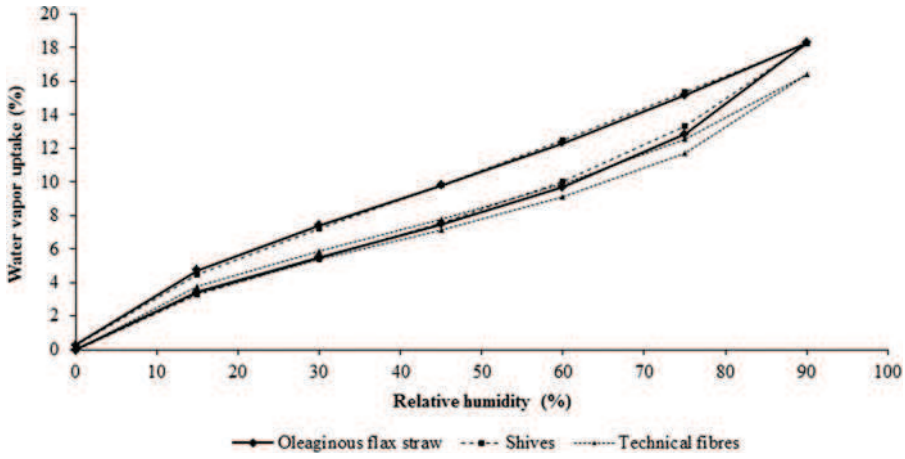

Figure 2. Water vapor sensitivity evaluation by DVS analysis for oleaginous flax straw, and shives and technical fibers generated after continuous fiber mechanical extraction from straw.

material surface, these being linked to the most polar groups inside shives, in particular the hydroxyl ones.

Solid particles of shives exhibit coarse stick shapes (Figure 1(a)). They revealed a 5.8-mm average length and a 1.1-mm average width, corresponding to a 6.2 aspect ratio (Table 2). Apparent and tapped densities were 117 and 131 kg/m^3, respectively (Table 3).

As a first pretreatment, shives were refined through twin-screw extrusion thanks to a thermo-mechanical fractionation. During refining of shives using the Clextral Evolum HT 53 machine, the current feeding the motor was 120 ± 13 A, and this corresponded to a 687 ± 77-W h/kg of dry matter specific mechanical energy. In parallel, the specific cooling and thermal energies were estimated to be 275 ± 3 W h/kg dry matter and 287 ± 8 W h/kg dry matter, respectively, corresponding to a 1249 ± 88-W h/kg dry matter total specific energy consumption. As for the thermomechanical pretreatment of rice straw fibers (Theng et al. 2017), cooling was needed at the level of the reversed screws situated, i.e., where the machine was completely filled and mechanical shear was the most important, and at the level of conveying screws positioned immediately upstream, thus preventing self-heating of the material. On the contrary, the heating power was required in the first part of the screw profile, i.e., in the feeding zone and immediately after water injection, to maintain the 110°C set temperature. Screw elements in this part were conveying screws and the bilobe paddle-screws used to disperse intimately water inside shives, for which filling was much lower (i.e., no material self-heating).

Table 2. Morphological characteristics of raw shives and extruded shives.

Material	Fiber length (µm)	Fiber diameter (or width) (µm)	Aspect ratio	Fines (%)
Raw shives	5804 ± 4013	1107 ± 669	6 ± 6	n.d.
Extruded shives	551 ± 24	20.7 ± 0.4	27 ± 1	58 ± 2

Results in the table correspond to the mean values ± standard deviations; n.d.: non-determined.

Table 3. Apparent and tapped densities of raw shives and extruded shives.

Material	Apparent density (kg/m^3)	Tapped density (kg/m^3)
Raw shives	117 ± 5	131 ± 4
Extruded shives	68 ± 4	88 ± 2

Results in the table correspond to the mean values ± standard deviations.

The 1.25 ± 0.09-kW h/kg dry matter total specific energy consumption was much higher than those observed during the thermomechanical defibration of both rice and coriander straws conducted from the same machine and with quite equivalent L/S ratios: 0.67 ± 0.10 kW h/kg dry matter for 1.02 L/S ratio (Theng et al. 2017) and 0.74 ± 0.03 kW h/kg dry matter for 1.0 L/S ratio (Uitterhaegen et al. 2017), respectively. This could be the consequence of the presence of some short technical fibers inside shives, and their entanglement contributed to a significant increase in the viscosity of the L/S mixture driven through the reversed screws. However, using a 0.08€/kW h cost of electricity in France in 2017, price for the thermomechanical pretreatment of shives was estimated to be of 0.10 ± 0.01€/kg dry matter, and this was much lower than the price of raw shives when proposed as animal litters: at least 0.25€/kg for shives from oleaginous flax, and until 0.45–0.55 €/kg for shives from the textile variety.

Morphological analysis of fibers inside extruded shives was conducted using a MorFi machine. Their average length and diameter were 551 and 20.7 µm, respectively, and this corresponded to a 26.7 aspect ratio (Table 2). As already observed in the case of coriander straw (Uitterhaegen et al. 2017), extrusion refining of shives thus resulted in an important increase in the fiber aspect ratio (from 6.2 to 26.7). As a consequence, extruded shives show lower densities than the raw ones: only 68 and 89 kg/m^3 for apparent and tapped densities, respectively, instead of 117 and 131 kg/m^3 for raw shives (Table 3). This indicated that fibers inside extruded shives were much more bulky than inside raw shives.

The stability of raw shives and extruded shives as a function of the increasing temperature was investigated by Thermo-Gravimetric Analysis (TGA). TGA and dTGA degradation curves of shives before and after twin-screw extrusion refining were perfectly equivalent (Figure 3(a) and (b), respectively). This suggested that the chemical composition of shives was the same before and after defibration. Indeed, thermomechanical pretreatment through twin-screw extrusion was carried out after water injection. However, water added corresponded only to a 1.0 L/S ratio, and this was insufficient to separate a filtrate from the extrudate. All molecules thus remain within the extruded material. Looking at the TGA degradation curves (Figure 3(a)), an initial mass loss was observed at about 100°C. This corresponded to the evaporation of water. Moisture contents of shives before and after twin-screw extrusion refining were 8–9% after conditioning (60% RH, 25°C), and this corresponded approximately to the initial mass loss. Thermal degradation of organic compounds inside shives then occurred in two successive stages. The main and first one took place in the 225–350°C temperature range, representing about 61% of the sample mass. Looking at data from literature, this corresponded to the simultaneous breakdown of water-soluble components, hemicelluloses, and then cellulose (Beaumont 1981; Evon, Amalia Kartika, and Rigal 2014b; Hatakeyama and Hatakeyama 2004; Hidayat et al. 2014; Lalou 1995; Schaffer 1973). A second degradation stage occurred between 375 and 475°C, representing a 21% weight loss of the sample. The latter corresponded essentially to the degradation of lignins (Evon et al. 2015b; Hidayat et al. 2014). However, because thermogravimetric analyses were conducted under air atmosphere, the second degradation stage may also involve the oxidation of primary degradation products (Uitterhaegen et al. 2016a, 2016b). At the end, a 1.5% residual weight was found, which corresponded to the minerals inside both samples.

From extruded shives, rectangular handsheets were formed (Figure 1(a)). They revealed a 246.6 ± 4.6-g/m^2 areal mass and a 1.44 ± 0.03-mm thickness, corresponding to a 170.9 ± 3.2-kg/m^3 sheet density. Fibers inside sheets were voluntarily parallelized during forming.

Influence of operating parameters on properties of fiberboards

Fiberboards were molded using the next thermo-pressing conditions: 200°C temperature, 19.7 MPa pressure, and 150 s time. The 200°C temperature was chosen below the beginning of thermal degradation of shives (Figure 3) and Biolignin™ (Theng et al. 2018), and above the lignin glass transition temperature (Theng et al. 2018) so as to reach a rubbery state for lignins during molding,

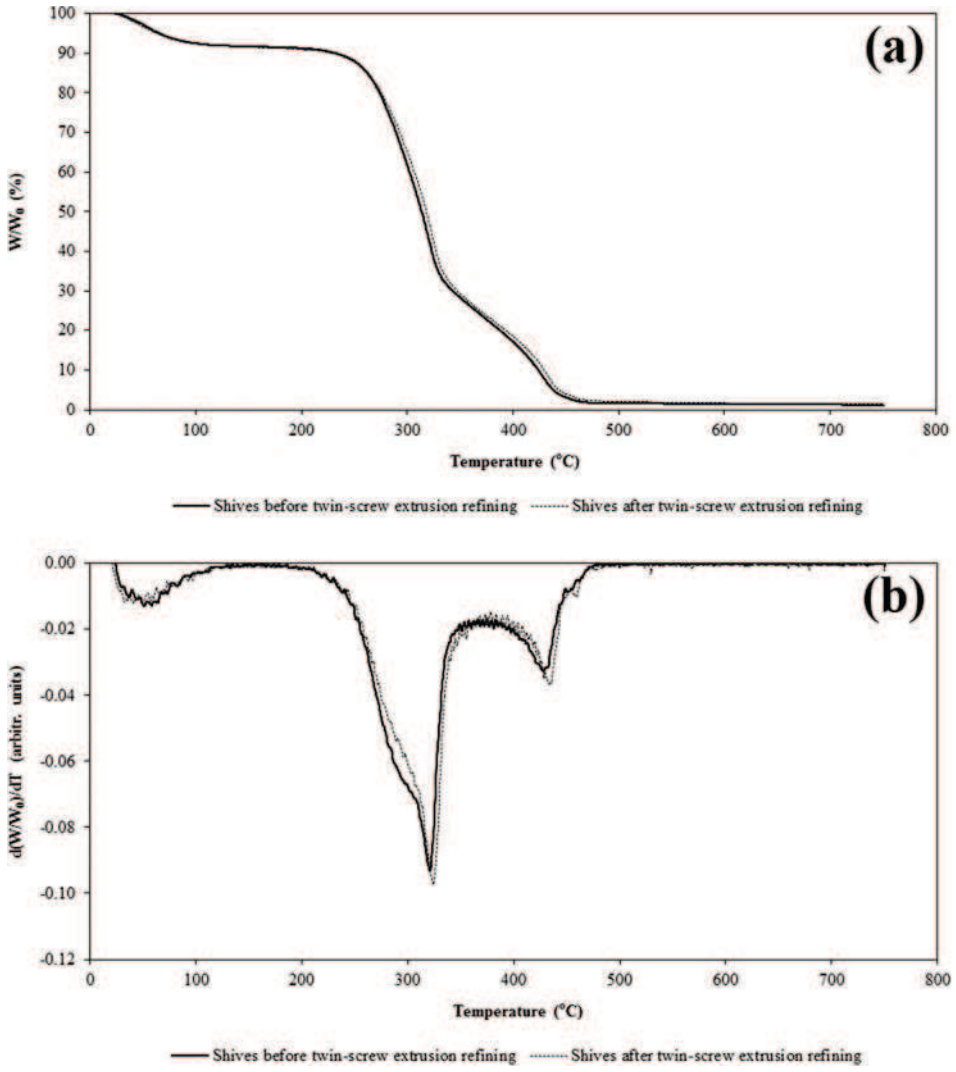

Figure 3. (a) TGA and (b) dTGA degradation curves of shives before and after twin-screw extrusion refining (W_0 and W, weights at the starting point and during scanning, respectively).

thus favoring the wetting of fibers. In parallel, pressure and time were chosen relatively high in comparison with values traditionally used for commercial particleboards produced in industry for indoor use (in general 5–6 MPa and 5–10 s/mm thickness, respectively). Indeed, when producing self-bonded fiberboards, the use of thermo-pressing with high temperature, pressure, and time is necessary to mobilize the natural binders (Tajuddin, Ahmad, and Ismail 2016), namely lignins in this case. As a consequence, fiberboards produced should reveal high density, making them hardboards. And, this could be a disadvantage in terms of handling. This is the reason why pressure and time were chosen here in the lower part of values used for other newly developed binderless boards produced at the laboratory scale (Theng et al. 2018; Uitterhaegen et al. 2016a, 2017, 2016b). Here, the objective was to minimize as much as possible the board density.

From the above molding conditions, three operating parameters were investigated. First, in addition to fiberboards made from raw shives, two different pretreatments were considered, i.e., (1) their thermomechanical defibration through twin-screw extrusion and (2) the handsheet

formation from extruded shives. Second, the addition of Biolignin™ was also tested. Characteristics of fiberboards were then measured. The five boards produced (Figure 1(b)–(f)) were all cohesive. Boards made from raw shives revealed a rough surface. On the contrary, the surface of boards originating from extruded shives and handsheets was smooth. In addition, boards where Biolignin™ was added were logically darker than the others. However, some black points appeared at their surface, and this suggested that Biolignin™ was not perfectly dispersed inside these two boards.

Despite its good machinability, RS board revealed very low mechanical properties (Table 4). Because cellulosic fibers and lignins were highly linked together inside raw shives, it seemed really difficult to correctly mobilize the ligneous binder during thermo-pressing, and this resulted in insufficient fiber wetting and board cohesion. When adding 25% Biolignin™ in proportion to raw shives (case of RSL board), bending properties and impact strength were much improved. In addition, both board density and surface hardness were also a little increased. These results confirmed that Biolignin™ fully played its role of exogenous binder inside RSL board, favoring an efficient bonding between solid particles from raw shives. Its binding ability was already evidenced inside boards from extruded rice straw (Theng et al. 2018).

Further improvement of bending properties and surface hardness was possible when using the extruded shives as the starting material for thermo-pressing (case of ES board). Indeed, thanks to the thermomechanical defibration pretreatment, lignins inside extruded shives were well separated from cellulose, and it was then much easier to mobilize them as a natural binder during hot pressing. In addition, because the aspect ratio of extruded fibers was much higher than inside raw shives (Table 2), their reinforcement ability was significantly improved. As a consequence, bending properties and surface hardness of ES board appeared higher than when Biolignin™ was added to raw shives (case of RSL board): +46% for flexural strength at break, +134% for elastic modulus, and +19% for Shore D (Table 4). The improvement in bending properties using extruded fibers has already been evidenced in a recent study using a pretreated coriander straw (Uitterhaegen et al. 2017).

As for raw shives, the addition of 25% Biolignin™ in proportion to extruded shives was also investigated (case of ESL board). However, and contrary to what was previously observed for raw shives, the addition of Biolignin™ did not help from a mechanical point of view in the case of extruded shives (Table 4). Indeed, when comparing ESL board with ES board, a reduction was observed for flexural

Table 4. Mechanical properties, thickness swelling, and water absorption of the five fiberboards manufactured by thermo-pressing, and specifications from French standard NF EN 312 of type P1 boards having a 3–6-mm thickness for flexural properties and internal bond strength.

Board type	RS	RSL	ES	ESL	HS	Type P1 boards (French standard NF EN 312)
Bending properties						
t (mm)	4.90 ± 0.24^{b}	5.56 ± 0.16^{a}	4.03 ± 0.03^{c}	4.80 ± 0.11^{b}	5.54 ± 0.13^{a}	3–6
d (kg/m^3)	1003 ± 20^{d}	1046 ± 17^{c}	1121 ± 16^{b}	1158 ± 23^{a}	789 ± 21^{e}	–
F (N)	12.5 ± 3.2^{c}	61.2 ± 7.1^{a}	47.5 ± 2.7^{b}	60.8 ± 9.8^{a}	7.3 ± 2.2^{c}	–
σ_f (MPa)	2.1 ± 0.7^{c}	8.0 ± 1.2^{b}	11.7 ± 0.8^{a}	10.3 ± 1.7^{a}	1.0 ± 0.3^{c}	11.5
E_f (MPa)	494 ± 158^{d}	682 ± 99^{c}	1598 ± 172^{a}	1233 ± 185^{b}	89 ± 35^{e}	–
Internal bond strength						
IB (MPa)	n.d.	n.d.	0.36 ± 0.03^{a}	0.30 ± 0.08^{a}	n.d.	0.31
Charpy impact strength						
W (mJ)	122 ± 22^{c}	373 ± 52^{a}	163 ± 17^{b}	206 ± 33^{b}	n.d.	–
K (kJ/m^2)	1.72 ± 0.34^{c}	4.69 ± 0.55^{a}	2.77 ± 0.31^{b}	2.97 ± 0.41^{b}	n.d.	–
Surface hardness						
Shore D (°)	60.7 ± 2.0^{c}	62.4 ± 0.2^{c}	74.4 ± 0.1^{a}	67.9 ± 1.3^{b}	46.9 ± 1.4^{d}	–
Thickness swelling and water absorption						
TS (%)	297.6 ± 27.5^{a}	294.2 ± 22.1^{a}	127.1 ± 15.9^{b}	122.7 ± 5.5^{b}	296.9 ± 5.5^{a}	–
WA (%)	143.9 ± 12.5^{b}	116.1 ± 16.7^{c}	102.9 ± 11.8^{cd}	89.7 ± 3.4^{d}	294.0 ± 21.0^{a}	–

Results in the table correspond to the mean values ± standard deviations; n.d.: non-determined.
Means in the same line with the same letter (a–e) are not significantly different at $P < 0.05$.
French standard NF EN 312, standard dedicated to the specifications for particleboards; type P1 boards, boards for general uses in dry conditions.

strength at break, elastic modulus, internal bond strength, and surface hardness: −12%, −23%, −16%, and −6%, respectively. This revealed that the only lignins inside the extruded shives, properly separated from the cellulosic fibers during extrusion refining and thus easily mobilized during thermo-pressing, were in a sufficient amount for a complete wetting of the surface area of extruded fibers. Therefore, ES board not only had better mechanical characteristics than the ESL one but it was also slightly less dense, which may be an advantage in terms of handling of large panels.

In terms of resistance to water, the higher the board density was, the higher was its water resistance (Table 4). In fact, an increase in the board density resulted in a reduction of its internal porosity, and this contributed to make it less water-sensitive. In particular, an important reduction in both TS and WA values (−58% and up to −38%, respectively) was obtained for boards from extruded shives, in comparison to results from raw shives boards. Because fines were generated during extrusion refining, these small particles contributed to a better filling of empty zones between fibers, thus reducing significantly the internal porosity. This rendered much more difficult the diffusion of water inside ES and ESL boards during soaking tests. The same phenomena, i.e., the increase in density and especially the decreases in TS and WA values, were also observed when Biolignin™ was added, the latter having the form of a powder made of small spherical particles. However, the improvement in the board resistance to water was much less significant in that case, the 25-g Biolignin™ added for RSL and ESL boards representing fewer fines than the ones inside extruded shives (58%) (Table 2).

In conclusion, ES board was the optimal one in terms of bending properties (11.7 MPa flexural strength at break and especially 1.6 GPa elastic modulus), internal bond strength (0.36 MPa), and Shore D surface hardness (74°). Manufactured from extruded shives and thus revealing a largely reduced internal porosity, it was also one of the two most resistant boards to water after 24 h soaking (127% TS and 103% WA). However, it was not the most resistant board to impact strength (Table 4). In fact, excessive panel rigidity significantly altered its impact resistance, and such phenomenon was previously reported in the literature (Evon et al. 2015b).

Looking at properties of HS board, its density was particularly low and this could be a real advantage in terms of subsequent handling. However, and although fibers inside sheets were oriented, its mechanical properties were particularly low (Table 4). In parallel, HS board was the most sensitive board to water. This was the consequence of a lack of adhesion of sheets to each other. Indeed, during bending tests, delamination between sheets was systematically observed. Two reasons could explain such a phenomenon. First, HS board was produced from sheets superimposed one on top of another and not from a bulk of fibers. And, the molding conditions suitable for bulk materials became certainly inappropriate in that case. Perhaps higher values for both temperature and especially pressure might solve this problem. Another reason could be the handsheet formation procedure itself. Indeed, when using the handsheet former, extruded shives were diluted in water, and the latter was then drained by centrifugal force. Perhaps some hemicelluloses and especially water-soluble components (e.g., free sugars) were removed from fibers. These chemicals are known for contributing to self-adhesion inside binderless boards (Tajuddin, Ahmad, and Ismail 2016), and this probably explains the lack of adhesion between layers. Low density HS board should nevertheless be usable for the thermal insulation of buildings (Evon et al. 2014a).

Bending properties were confirmed by DMTA analysis (Figure 4). Indeed, when observing the thermomechanical properties of the five fiberboards from −50 to 120°C, the higher the board bending properties at ambient temperature are, the higher are the storage moduli (E'). The highest E' values in this temperature range were those of ES board, meaning that the latter revealed the best internal cohesion. As a reminder, ES board also had the best mechanical properties at 25°C (Table 4). Looking specifically at DMTA analysis of this optimal fiberboard, no significant temperature transition occurred between −50 and 50°C. This indicated that no phase change took place in this temperature range. This also means that the natural binders inside extruded shives, especially lignins, still ensure the board cohesion and the entanglement of cellulosic fibers serving as reinforcement. Then, a first transition was observed from 50 to 110°C, corresponding to a rapid decrease in the storage modulus (Figure 4(a)), which simultaneously produced a peak in the DMTA loss factor (tan

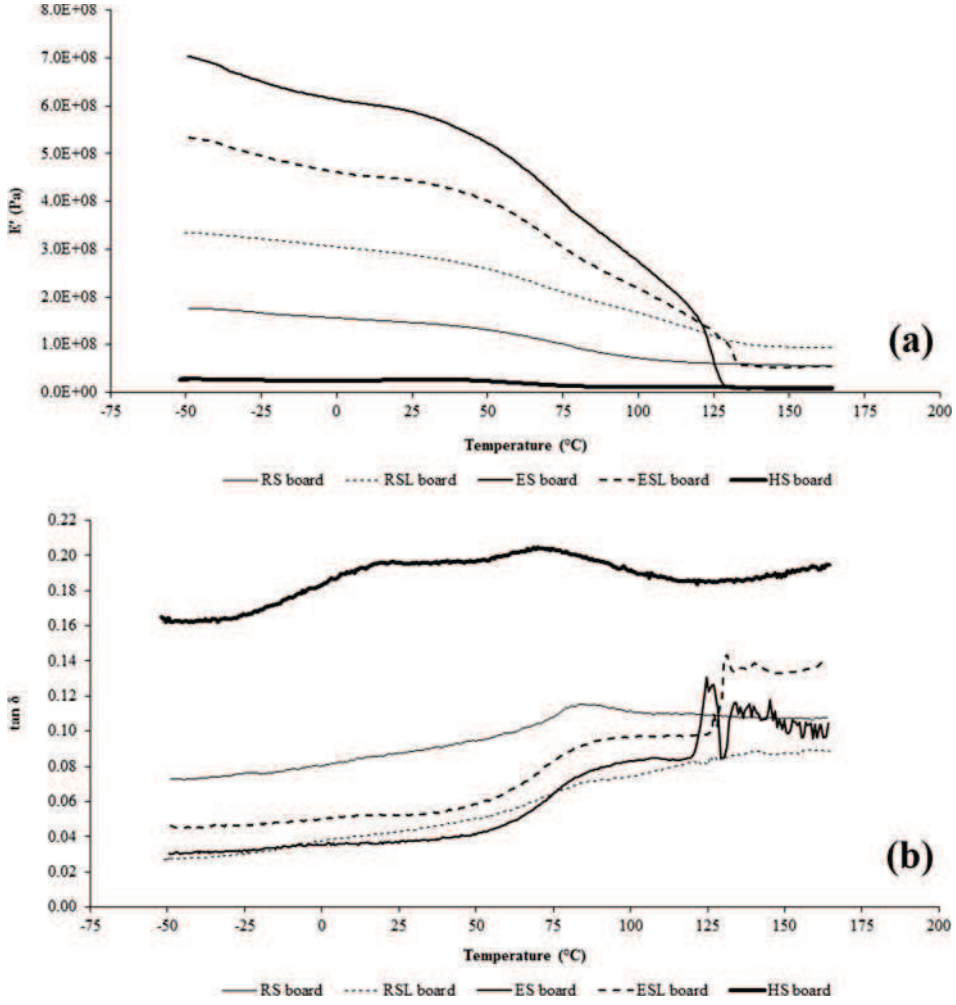

Figure 4. DMTA curves of RS, RSL, ES, ESL, and HS boards: (a) storage modulus (E') and (b) loss factor (tan δ).

δ) curve (Figure 4(b)). Thus, it is reasonable to assume that this transition could be associated to the glass transition of natural binders inside extruded shives having the lowest molecular weights, i.e., water-soluble components in priority and then hemicelluloses. The corresponding glass transition temperature (about 95–100°C) was identified from the midpoint in the loss factor peak. Then, after another rapid decrease, the storage modulus of ES board became minimal for temperatures higher than 130°C. The same phenomenon was also observed in the case of ESL board. This suggests that the glass transition of lignins originating from shives and liberated thanks to the extrusion thermo-mechanical pretreatment already occurred in this temperature range. Thus, lignins were then in a rubbery state and the cohesion of ES board was no longer ensured by its own lignin-based resin. In conclusion, because no phase change occurred inside ES board up to 50°C, not to exceed this temperature in its use conditions will guarantee a good cohesion for this optimal board.

Possible uses of optimal fiberboard

Fiberboard having the best mechanical properties of the entire study was ES board, manufactured from extruded shives without addition of any supplementary lignin amount (Table 4). This

confirmed the great interest of the extrusion refining pretreatment of shives before molding, as previously evidenced in the case of coriander straw (Uitterhaegen et al. 2017). Even if such thermomechanical defibring resulted in an extra cost representing about 40% of the economic value of raw shives, its interest for the properties of the resulting ES board was incontestable.

First, from a morphological point of view, extrusion refining led to an important increase in the mean aspect ratio of fibers inside extruded shives (Table 2). And, this contributed to better mechanical reinforcement inside boards. In addition, fines generated during extrusion made possible the filling of empty zones between fibers inside ES board, leading not only to a denser board but also to additional bonds between fines and fibers.

Second, extrusion refining contributed to a complete disassembly of the starting lignocellulosic material. This led to an efficient separation between cellulosic fibers and lignins inside the extruded material, thus facilitating the mobilization of the ligneous binder during thermo-pressing. In addition, when using extruded shives, the doubling of the lignin amount (i.e., ESL board) did not improve the board mechanical properties despite a little higher density. This confirmed once again that lignins from shives were efficiently mobilized during molding and probably more compatible with cellulosic fibers than Biolignin™.

Lastly, extrusion refining contributed also to the disassembly of other molecules inside shives, in particular water-soluble components and especially hemicelluloses. It is reasonable to assume that those compounds could also contribute to self-bonding inside ES board (Tajuddin, Ahmad, and Ismail 2016).

The ES optimal fiberboard perfectly complied with French standard NF EN 312 (standard dedicated to the specifications for particleboards), type P1 (i.e., boards for general uses in dry conditions) for flexural properties and internal bond strength (recommendations of 11.5 and 0.31 MPa for flexural strength at break and internal bond strength, respectively, for boards with a 3–6-mm thickness). Thus, from such mechanical properties and despite a quite limited resistance to water, this optimal board could be used for example (1) as an interlayer sheet for pallets in the handling and storage industry, (2) for the manufacture of intermediate containers, or (3) in the building trade for more durable uses (e.g., floor underlayers, interior partitions, ceiling tiles, etc.).

For future work, an observation of ES optimal fiberboard through the tomography technique will allow to study the density profile of the panel, from its middle to its outer faces. From tomograms, it will thus be possible to study the board's homogeneity in terms of porosity distribution, which can be a key issue for materials molded using hot pressing. This would undoubtedly give much more information about the board's internal structure. In addition, successive soaking procedures in water, all preceded by the board drying, would be interesting from a water resistance point of view. Indeed, several soaking and drying cycles are usually conducted to determine the stability to water of commercial panels on the long term, especially the ones to be used in wet conditions, and the incidence of these repeated cycles on their flexural properties.

Conclusion

Representing more than 50% of the oleaginous flax straw dry mass, shives constitute the major by-product generated during the continuous mechanical extraction of technical fibers. In this study, a new application was investigated for shives, i.e., the production of renewable and binderless fiberboards through thermo-pressing.

Cohesive fiberboards were produced successfully, even with no addition of Biolignin™, cellulosic fibers and lignins from shives acting as mechanical reinforcement and naturel binder, respectively. The best mechanical properties (11.7 MPa flexural strength at break, 1.6 GPa elastic modulus, 0.36 MPa internal bond strength, 2.8 kJ/m^2 Charpy resilience, and 74° Shore D surface hardness) were obtained from shives which were primarily refined through twin-screw extrusion. This thermomechanical pretreatment contributed to an important increase in the fiber aspect ratio and

facilitated also the subsequent mobilization of lignins from shives during hot pressing. In addition, extrusion refining much improved the resistance to water of fiberboards.

From such characteristics and looking at French standard NF EN 312, the optimal board would be suitable for general uses in dry conditions (i.e., type P1 board). It would be potentially usable as an interlayer sheet for pallets, for the manufacture of containers, or in the building trade (e.g., floor underlayers, interior partitions, ceiling tiles, etc.).

For the future, characteristic properties of binderless boards from extruded shives will need to be improved. First, increasing both pressure and time during thermo-pressing should increase the board mechanical properties, even if it could also contribute to an increase in its density. An improvement in its water resistance will be also required to authorize its use in wet conditions. Additional processes after hot pressing (e.g., coating, preheating, chemical, or steam treatment) would probably improve this dimensional stability parameter.

Acknowledgments

The authors would like to express their sincere gratitude to Ovalie Innovation (Auch, France) for supplying the batch of non-retted oleaginous flax straw used for the purpose of this study, and to CIMV company (Labège, France) for supplying Biolignin™. The authors would also like to thank Marc Delgado-Aguilar (Laboratori d'Enginyeria Paperera i Materials Polímers (LEPAMAP) research group, University of Girona, Spain) for conducting the extruded fiber morphology determination using the MorFi technique, Dominique Moineau from TechPap company (Saint-Martin d'Hères, France) for forming handsheets from extruded shives using an ADF automated dynamic handsheet former, and Othmane Merah (Laboratoire de Chimie Agro-industrielle, Université de Toulouse, France) for performing the statistical analyses.

References

ADEME. 2011. Report: Assessment of natural fiber availability in France. http://www.ademe.fr/sites/default/files/assets/documents/76290_12_evaluation_dispo_accessibilite_fibers_veg_usages_materiaux.pdf.

Anglès, M. N., F. Ferrando, X. Farriol, and J. Salvadó. 2001. Suitability of steam exploded residual softwood for the production of binderless panels. Effect of the pre-treatment severity and lignin addition. *Biomass and Bioenergy* 21:211–24.

Anglès, M. N., J. Reguant, D. Montané, F. Ferrando, X. Farriol, and J. Salvadó. 1999. Binderless composites from pretreated residual softwood. *Journal of Applied Polymer Science* 73:2485–91.

Beaumont, O. 1981. Pyrolyse extractive du bois. Ph.D. Thesis, École Nationale Supérieure des Mines de Paris, Paris, France.

Evon, Ph., I. Amalia Kartika, and L. Rigal. 2014b. New renewable and biodegradable particleboards from jatropha press cakes. *Journal of Renewable Materials* 2 (1):52–65.

Evon, Ph., V. Vandenbossche, P. Y. Pontalier, and L. Rigal. 2014a. New thermal insulation fiberboards from cake generated during biorefinery of sunflower whole plant in a twin-screw extruder. *Industrial Crops and Products* 52:354–62.

Evon, Ph., J. Vinet, L. Labonne, and L. Rigal. 2015b. Influence of thermo-pressing conditions on mechanical properties of biodegradable fiberboards made from a deoiled sunflower cake. *Industrial Crops and Products* 65:117–26.

Evon, Ph., J. Vinet, M. Rigal, L. Labonne, V. Vandenbossche, and L. Rigal. 2015a. New insulation fiberboards from sunflower cake with improved thermal and mechanical properties. *Journal of Agricultural Studies* 3 (2):194–211.

Felby, C., J. Hassingboe, and M. Lund. 2002. Pilot-scale production of fiberboards made by laccase oxidized wood fibers: Board properties and evidence for cross-linking of lignin. *Enzyme and Microbial Technology* 31:736–41.

Felby, C., L. S. Pedersen, and B. R. Nielsen. 1997. Enhanced auto adhesion of wood fibers using phenol oxidases. *Holzforschung* 51:281–86.

Felby, C., L. G. Thygesen, A. Sanadi, and S. Barsberg. 2004. Native lignin for bonding of fiber boards: Evaluation of bonding mechanisms in boards made from laccase-treated fibers of beech (*Fagus sylvatica*). *Industrial Crops and Products* 20:181–19.

Gamon, G., Ph. Evon, and L. Rigal. 2013. Twin-screw extrusion impact on natural fiber morphology and material properties in poly(lactic acid) based biocomposites. *Industrial Crops and Products* 46:173–85.

Gazagnes, E., C. Magniont, and G. Escadeillas. 2009. Matériau composite de construction incorporant de la chènevotte de chanvre. Brevet FR 2.946.640.

Hatakeyama, T., and H. Hatakeyama. 2004. *Thermal properties of green polymers and biocomposites*. Dordrecht: Kluwer Academic Publishers.
Hidayat, H., E. R. P. Keijsers, U. Prijanto, J. E. G. van Dam, and H. J. Heeres. 2014. Preparation and properties of binderless boards from Jatropha curcas L. seed cake. *Industrial Crops and Products* 52:245–54.
Lalou, A. 1995. Mise au point d'un procédé d'extraction des hémicelluloses à partir d'un substrat végétal lignocellulosique: application au cas des coques de tournesol. Ph.D. Thesis, INP, Toulouse, France.
Ouagne, P., B. Barthod-Malat, Ph. Evon, L. Labonne, and V. Placet. 2017. Fiber extraction from oleaginous flax for technical textile applications: Influence of pre-processing parameters on fiber extraction yield, size distribution and mechanical properties. *Procedia Engineering* 200:213–20.
Pillin, I., A. Kervoelen, A. Bourmaud, J. Goimard, N. Montrelay, and C. Baley. 2011. Could oleaginous flax fibers be used as reinforcement for polymers? *Industrial Crops and Products* 34:1556–63.
Pintiaux, T., D. Viet, V. Vandenbossche, L. Rigal, and A. Rouilly. 2015. Binderless materials obtained by thermocompressive processing of lignocellulosic fibers: A comprehensive review. *BioResources* 10:1915–63.
Quintana, G., J. Velásquez, S. Betancourt, and P. Gañán. 2009. Binderless fiberboard from steam exploded banana bunch. *Industrial Crops and Products* 29:60–66.
Rennebaum, H., E. Grimm, K. Warnstorff, and W. Diepenbrock. 2002. Fiber quality of linseed (*Linum usitatissimum* L.) and the assessment of genotypes for use of fibers as a by-product. *Industrial Crops and Products* 16:201–15.
Schaffer, E. L. 1973. Effect of pyrolytic temperatures on the longitudinal strength of dry Douglas-fir. *Journal of Testing and Evaluation* 1 (4):319–29.
Tajuddin, M., Z. Ahmad, and H. Ismail. 2016. A review of natural fibers and processing operations for the production of binderless boards. *BioResources* 11:5600–17.
Theng, D., G. Arbat, M. Delgado-Aguilar, B. Ngo, L. Labonne, Ph. Evon, and P. Mutjé. 2017. Comparison between two different pretreatment technologies of rice straw fibers prior to fiberboard manufacturing: Twin-screw extrusion and digestion plus defibration. *Industrial Crops and Products* 107:184–97.
Theng, D., G. Arbat, M. Delgado-Aguilar, B. Ngo, L. Labonne, Ph. Evon, and P. Mutjé. 2018. Production of fiberboards from rice straw thermo-mechanical extrudates by thermopressing: Influence of fiber morphology, water addition and lignin content. *European Journal of Wood and Wood Products* under review.
Tomljenovic, A., and M. Erceg. 2016. Characterisation of textile and oleaginous flax fibrous and shives material as potential reinforcement for polymer composites. *Tekstilec* 59 (3):350–66.
Uitterhaegen, E., L. Labonne, O. Merah, T. Talou, S. Ballas, T. Véronèse, and Ph. Evon. 2016a. Optimization of thermopressing conditions for the production of binderless boards from a coriander twin-screw extrusion cake. *Journal of Applied Polymer Science* 134 (13):44650.
Uitterhaegen, E., L. Labonne, O. Merah, T. Talou, S. Ballas, T. Véronèse, and Ph. Evon. 2017. Impact of thermomechanical fiber pre-treatment using twin-screw extrusion on the production and properties of renewable binderless coriander fiberboards. *International Journal of Molecular Sciences* 18 (7):1–20.
Uitterhaegen, E., Q. H. Nguyen, O. Merah, C. V. Stevens, T. Talou, L. Rigal, and Ph. Evon. 2016b. New renewable and biodegradable fiberboards from a coriander press cake. *Journal of Renewable Materials* 4 (3):225–38.
Van Soest, P. J., and R. H. Wine. 1967. Use of detergents in the analysis of fibrious feeds. IV. Determination of plant cell wall constituents. *Journal of AOAC International* 50:50–55.
Van Soest, P. J., and R. H. Wine. 1968. Determination of lignin and cellulose in acid detergent fiber with permanganate. *Journal of AOAC International* 51:780–84.
Velásquez, J. A., F. Ferrando, X. Farriol, and J. Salvadó. 2003. Binderless fiberboard from steam exploded miscanthus sinensis. *Wood Science and Technology* 37:269–78.
Xu, J., R. Widyorini, H. Yamauchi, and S. Kawai. 2006. Development of binderless fiberboard from kenaf core. *Journal of Wood Science* 52:236–43.